Spectroscopic analysis of erbium-doped silicon and ytterbium-doped indium phosphide

de Maat-Gersdorf, I.

Publication date
2001

Citation for published version (APA):
de Maat-Gersdorf, I. (2001). *Spectroscopic analysis of erbium-doped silicon and ytterbium-doped indium phosphide*. [Thesis, fully internal, Universiteit van Amsterdam].

Chapter 2

Photoluminescence measurements on erbium-doped silicon

Abstract

Photoluminescence measurements of erbium-doped float-zone silicon, Czochralski-grown silicon and silicon oxide are reported. A striking similarity between the spectra of the latter two (oxygen-containing) materials is established. The structure of the spectra can be understood as being due to the appearance of phonon replicas together with crystal-field-induced splitting. At higher temperatures an anti-Stokes line and so-called hot lines were observed. The analysis is consistent with the model of erbium impurities that are surrounded by oxygen atoms on nearest-neighbour positions in an arrangement with cubic and/or lower symmetry.

2.1 Introduction

Rare-earth doping of semiconductors has been intensively investigated with a view to its application in optoelectronic devices. The presence of an incompletely filled 4f shell offers the attractive possibility of induced intra-shell excitations, largely independent of the surrounding environment. Sharp atomic-like spectra can consequently be generated, with their wavelengths being practically controlled by the dopant itself, rather than by the host crystal. Recently, considerable interest and research effort has been directed at erbium-doped silicon. This is for two main reasons: first the characteristic 4f transitions of the erbium ion in the 1.5 µm range coincide with the optical window of glass fibres currently used for telecommunications, and secondly, such a system can be easily integrated with devices manufactured using the highly successful standard silicon technology.

Studies of silicon, silica, GaAs and InP doped with erbium have been reported [2.1–2.5]. The majority of the studies on the Si:Er system concentrate on the practical aspect of how to

obtain the maximum intensity of photoluminescence or electroluminescence at as high a temperature as possible, preferably room temperature. In order to achieve this goal, non-equilibrium doping procedures have been explored [2.2] and the influence of different "co-activators" on the erbium luminescence has been investigated [2.6]. The more fundamental aspects behind the excitation and de-excitation mechanisms and the microscopic features of the defect created by an erbium ion imbedded in the silicon lattice have, however, not been studied in sufficient detail. One may expect that only with a deeper understanding of the physics of the light-emission process the highly efficient erbium-based silicon optical devices can be obtained.

The current study aims to analyse the photoluminescence (PL) spectrum of the erbium atom in various host crystals. The influence of the crystal field on the structure of the spectrum, i.e., the number and intensity of the emission lines, is considered. To this end the luminescence spectra as obtained at liquid-helium temperature are analysed for erbium ions imbedded in float-zone and Czochralski-grown silicon and in silicon oxide.

In silica glass, extended X-ray absorption fine structure (EXAFS) measurements have been performed by Marcus and Polman [2.3]. They found that the majority of the erbium impurities in silica has a local structure of six oxygen first neighbours at a distance of 2.28 Å and a next-nearest neighbour shell of silicon at 3.1 Å. At room temperature the PL spectrum of erbium-doped silica showed a line at 1535 nm with a shoulder at 1550 nm [2.3]. At lower temperatures only a very broad band at 1540–1600 nm has been reported [2.7].

The same technique, EXAFS, has been used to unravel the structure around the erbium in float-zone (FZ) and Czochralski (Cz) silicon [2.8]. The float-zone samples have an oxygen concentration of two orders of magnitude lower than the Czochralski silicon samples. Bulk compounds of $ErSi_2$ and Er_2O_3 were used as a reference.

Er_2O_3 has a bixbyite structure with 32 erbium ions and 48 oxygen ions in a cubic unit cell. There are two sites: 24 of the erbium ions have a twofold rotational symmetry (C_2) and 8 have a threefold rotation-inversion symmetry (C_{3i}). The erbium ions have six oxygen nearest neighbours. The oxygen atoms are located almost on the corners of a cube with the erbium at the centre, in C_2 two oxygen atoms are missing along a face diagonal, in C_{3i} along a <111> direction [2.9]. The energy levels of the ground state of the erbium ion at a C_2 site are schematically given in figure 2.1 [2.10]. Because of this low symmetry and the two different sites one would expect 16 lines in the photoluminescence spectrum at 4 K.

A striking similarity was found between the FZ Si:Er sample and $ErSi_2$ and between the Cz Si:Er sample and Er_2O_3, respectively. A first-neighbour shell for FZ Si:Er of twelve silicon atoms and a first-neighbour shell for Cz Si:Er of six oxygen atoms at a distance of 2.25 Å was concluded.

30

It appears, therefore, that Er^{3+} is surrounded by oxygen in Czochralski silicon, silica and erbia, but there is still some uncertainty about the symmetry of the defect and even the number of oxygen ligands in the first-neighbour shell of the luminescent centres may be questioned. It is also not well established whether the erbium centres as observed in EXAFS and luminescence are the same.
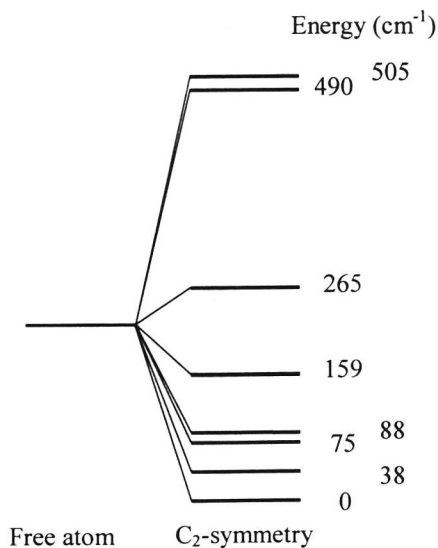

Figure 2.1 *The energy level diagram of erbium in Er_2O_3, state $^4I_{15/2}$, and its eightfold splitting at a C_2-symmetry site, (after [2.11]).*

Investigating photoluminescence in an erbium-doped (presumably Czochralski-grown) silicon sample, Tang *et al.* [2.2] report the observation of two different erbium sites: a thermally stable interstitial with cubic symmetry giving five lines in PL due to the fivefold splitting of the $^4I_{15/2}$ ground state and an unstable interstitial having non-cubic symmetry with a more complicated PL spectrum. In table 2.1 the transitions of the lowest energy level of the first excited state $^4I_{13/2}$ to the energy levels of the ground state $^4I_{15/2}$ or Er^{3+}, electron configuration $4f^{11}$, are given, for silicon at a cubic and a non-cubic site [2.2]. This transition in the free atom is at 1541.8 nm (804.16 meV) [2.11].

Michel *et al.* [2.6] observed photoluminescence of float-zone and Czochralski-grown silicon, doped with erbium and co-doped with nitrogen and carbon. The Czochralski samples all showed the lines observed by Tang *et al.* [2.2] and some small extra lines depending on the co-dopant. It was shown that only a maximum of ten percent of the erbium is optically active, these being the erbium atoms surrounded by oxygen and consistent with a T_d symmetry.

Table 2.1 *Overview of the positions of the luminescence lines as in figure 2.2 and a comparison with line positions known from the literature. Wavelengths are given in nm.*

	This work			Reference [2.2]		Reference [2.12]	
Label	FZ Si	Cz Si	SiO$_2$	Cz Si Cubic	Cz Si Non-cubic	FZ Si Cubic	Cz Si Non-cubic
A	1538	1536.9	1536.6	1537.5	1537.5	1537.3	1536.7
B	1543	1538.2	1539.5		1540.0		
	1545	1546					1544.9
C	1550	1550.7	1550.8				
	1552				1553.3		1553.3
D	1556	1555.3	1555.2	1556.0		1556.2	
E	1562						
	1567.5	1568.2	1567		1570.0		1566.5
F	1574.4	1574.6	1574.2	1575.0		1575.4	
G		1581.4			1581.2		1583.6
			1592				
H		1597.8	1597.5	1597.5	1597.5	1598.6	
I		1602.7	1608				1605.4
J					?		1619.9
K		1642.8	1641	1640		(1633.5)	
L					?		
M		1667	1667				

The co-dopant (N, C) increased the luminescence at 4.2 K with a factor of 5 and at room temperature with a factor of 10. The energies in the PL spectrum do not change much upon co-implantation; therefore the increase of luminescence is probably due to enhancement of the excitation or the blocking of a non-radiative de-excitation mechanism [2.6].

The float-zone samples showed a different spectrum with a broad band around 1540 nm and some more lines with a low intensity. This was explained by a much smaller crystal-field splitting, 50 cm^{-1}, instead of the 430 cm^{-1} in Cz Si. Coffa *et al.* [2.13] studied the temperature dependence and quenching processes in Cz Si:Er and found two different classes of optically active Er sites. One site does not depend on the oxygen concentration, decays slowly and decreases rapidly when the temperature is increased. The other site is dominant at higher

temperatures, decays fast and its photoluminescence is strongly increased by the presence of oxygen.

2.2 Experimental method

Two kinds of silicon, with low and high oxygen concentration, respectively, were used in this experiment:

- Float-zone silicon with an implantation of 1.6×10^{15} cm^{-2} Er and annealed at 450 °C for 1 hour and at 550 °C for 2 hours,

- Czochralski silicon with a 1 MeV implantation of 1×10^{13} cm^{-2} Er and subsequent annealing in a chlorine-containing atmosphere.

The silica used in this experiment was implanted with 1.7×10^{15} cm^{-2} Er and annealed at 900 °C for 30 minutes.

The samples are mounted in an Oxford Instruments cryostat (Spectromag 4). Most of the experiments were performed with the samples immersed in liquid helium. The sample room is connected with a helium dewar by a capillary tube with a needle valve. This helium dewar contains a split-coil superconducting magnet with a maximum field of 6 tesla. By pumping on the liquid helium in the sample space, temperatures below the λ-point (2.17 K) can be reached (as low as 1.5 K). By adjusting the helium gas flow from the main bath through the capillary tube, temperatures above 4.2 K are obtainable. Temperature control within 0.1 K is achieved by PID regulation (Oxford Instruments DTC2) of the current through a heater wound on a copper block on which the samples are glued. The temperature, measured with a RhFe metallic resistor using a four-point-probe configuration, is read directly in kelvin by passing the sensor output through a lineariser with a characteristic inverse to that of the sensor. The sample could be heated up to about 100 K in order to measure temperature dependencies of the spectra. The luminescence was excited with a CW argon-ion laser (Spectra-Physics Stabilite 2016-05s) with a maximum power output of 5 W, operating at a wavelength of 514.5 nm; an interference filter was used to avoid spurious plasma lines. An on–off light chopper was placed between light source and sample. The emerging luminescence light was collected from the laser-irradiated side. It was dispersed by a high-resolution 1.5-m F/12 monochromator (Jobin-Yvon THR-1500) with a 600 grooves/mm grating blazed at 1500 nm. Optical filters were placed in front of the monochromator entrance slit in order to select the emission bands of interest. The luminescence was detected by a liquid-nitrogen-cooled germanium detector (North Coast EO-817). The detector output was amplified using conventional lock-in (Keithley 840) techniques at the chopper frequency, with optional

filtering to remove the spikes due to cosmic radiation. The lock-in output was digitized and fed into a computer for further data processing.

2.3 Experimental results

The photoluminescence spectra of Cz Si:Er, FZ Si:Er and SiO_2:Er in the spectral range from 1530–1650 nm (810–751 meV) at liquid-helium temperature are given in figure 2.2. The positions of the lines and a comparison with some spectra of cubic and non-cubic erbium defects in silicon produced under different conditions of implantation dose and energy and subsequent annealing temperature as reported in the literature [2.2, 2.6, 2.12] are given in table 2.1. Since a new interpretation will be discussed for the origin of the luminescence lines, they are provisionally labelled as line A to line M.

The weak luminescence spectrum of FZ Si:Er shows a broad band of approximately 6 nm width around 1537 nm and several more lines which are hardly resolved; the lowest-energy line is observed at 1574.4 nm. The ten times stronger spectrum of Cz Si:Er shows as its most dominant feature two overlapping lines, at 1536.9 and at 1538.2 nm, and some smaller, sharp lines at larger wavelengths. At 1642.8 and 1667 nm two more weak lines are observed; part of the reason why these lines are weak is the decreased sensitivity of the germanium detector at wavelengths longer than 1600 nm. The luminescence spectrum of SiO_2:Er also consists of several sharp lines and some more incompletely resolved lines located between 1537 and 1540 nm. The lowest-energy lines at 1641 and 1667 nm are also observed. The similarities between the spectra of Cz Si:Er and SiO_2:Er are striking. The behaviour of the luminescence lines, i.e. the dependence of their absolute and relative intensities and energies on excitation power, chopper frequency, temperature and magnetic field, was measured. Results of the introductory studies are summarised as follows. The relative intensities of the lines do not change at all with excitation power; the absolute intensity increases only from 0 to 50 mW and then remains constant up to 400 mW, which is the maximum available excitation power in the experiment. All the luminescence lines of erbium are strongly dependent on the chopper frequency; the optimum being around 30 Hz; when changed to 830 Hz the intensity drops to 3 percent of that detected at 30 Hz. Since the responses of detector and amplifier are flat in this frequency range, the decrease reflects the long lifetime, of milliseconds, of the decaying state [2.13]. The lines A, D and F are relatively more frequency dependent than the lines B and C. The lines A, D, F and H can still be seen at 77 K and disappear only around 120 K, where they start to overlap and form a broad structure with a shoulder from 1450 to 1650 nm, the relative intensities between A, D, F and H are rather stable.
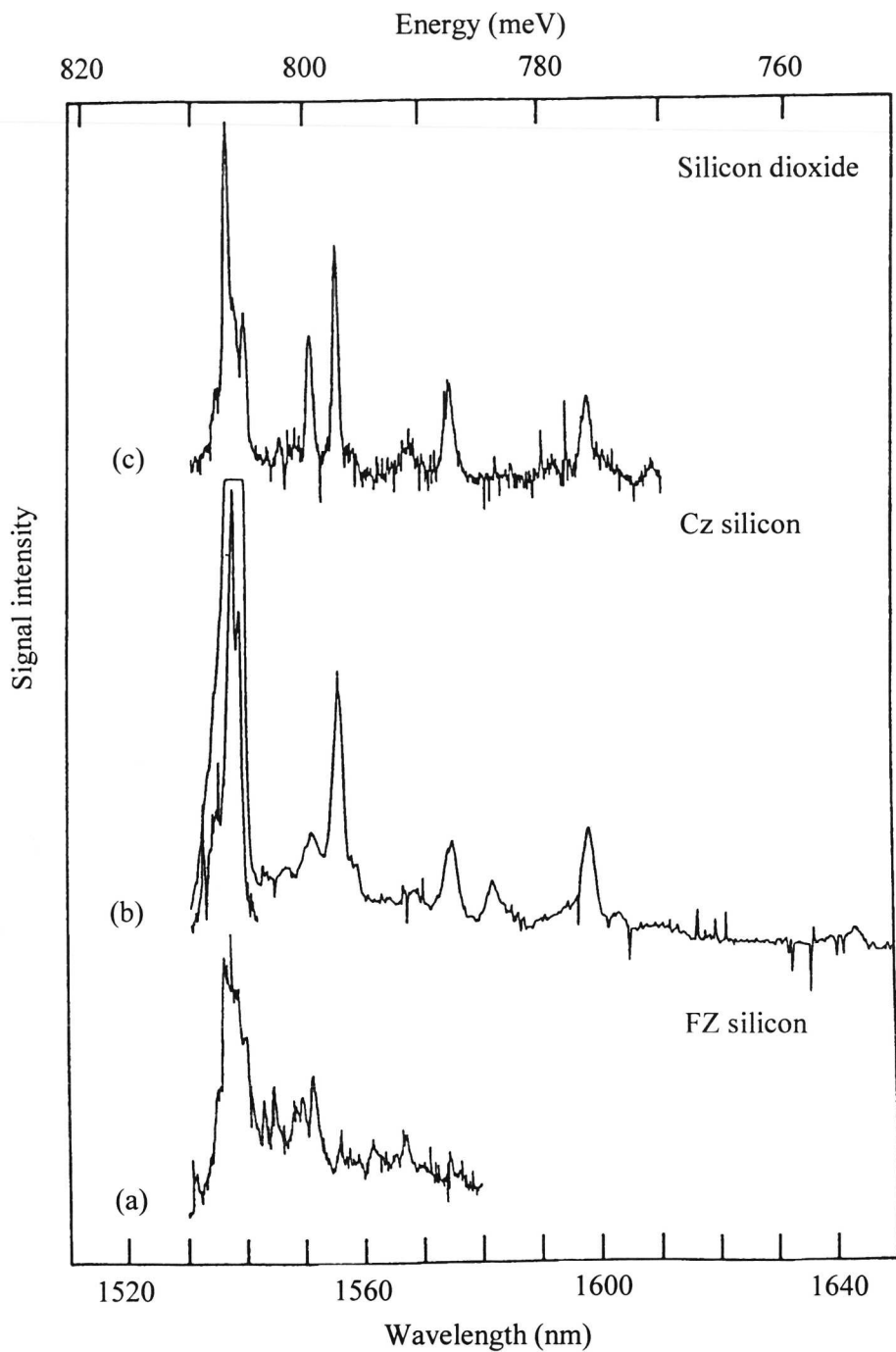
Figure 2.2 *Photoluminescence spectra, measured at 4.2 K, of FZ Si, Cz Si and SiO₂, doped with erbium. (Spectra were also recorded with on-line filtering, removing the spurious spikes. Alternatively, off-line digital filtering produced smoother spectra.)*

Line C and the other small lines are completely gone at 77 K. At higher temperatures a new PL line at 1517.8 nm and several high-energy shoulders at ≈5 meV are observed. The lines A, D and F are hardly influenced by magnetic fields up to 5 tesla, whereas the other lines broaden and disappear. The luminescence intensities of Cz Si:Er and SiO_2:Er behave identically in all these experiments; no energy shift of any line is observed.

The spectrum of Er_2O_3 shows a variety of effects on change of the temperature, see figure 2.3. At 300 K a great number of lines can be seen in the region from 1450 to 1650 nm. Upon decrease of temperature some lines split into two; others shift or completely disappear. The spectrum at 4.2 kelvin shows a very sharp, very strong line at 1547 nm, a weaker line at 1544 nm, and some, relatively, very weak lines around 1560 nm. When exposed to atmosphere the high- and low-temperature spectra disappear completely within a week. The two main lines get broader and smaller when exposed to a magnetic field up to 5 tesla.

2.4 Discussion

2.4.1 Ligand oxygen atoms

The spectra of Cz Si:Er and SiO_2:Er look very much the same. Although the relative intensities differ, the positions of the lines in the spectra agree, as can be seen in figure 2.2. This is very surprising since the amount of oxygen in the two materials differs by orders of magnitude. Whereas it is not possible to accommodate an erbium ion in SiO_2 without oxygen in its vicinity, the formation of an oxygen-surrounded erbium centre in Cz silicon requires migration of oxygen over long distances. Besides, Cz Si is crystalline and silica is a glass. Yet, in view of other evidence, the generally assumed role of oxygen in forming the luminescent centre should not easily be abandoned. The spectra of the FZ silicon, basically without oxygen, show a much smaller splitting. This can be understood from the absence of oxygen-related ligand fields.

Independent support of oxygen-related models is derived from an erbium spectrum observed in GaAs [2.4], which is identical to that arising from Er_2O_3. The two spectra are compared in figure 2.3. The GaAs:Er spectrum disappears by mechanical polishing, removing an about 1 μm thick surface layer. Zeeman measurements reveal that the symmetry is cubic, a g factor of 0.85 is deduced from the isotropic splitting of the line at 1549 nm. The luminescence is restored by heat treatment at 850 °C. Apparently in this case the luminescence arises from a centre located near the surface and possibly formed by oxidation. Since our experiments are performed with Er_2O_3 powder in a quartz ampoule, a large surface area will be available for
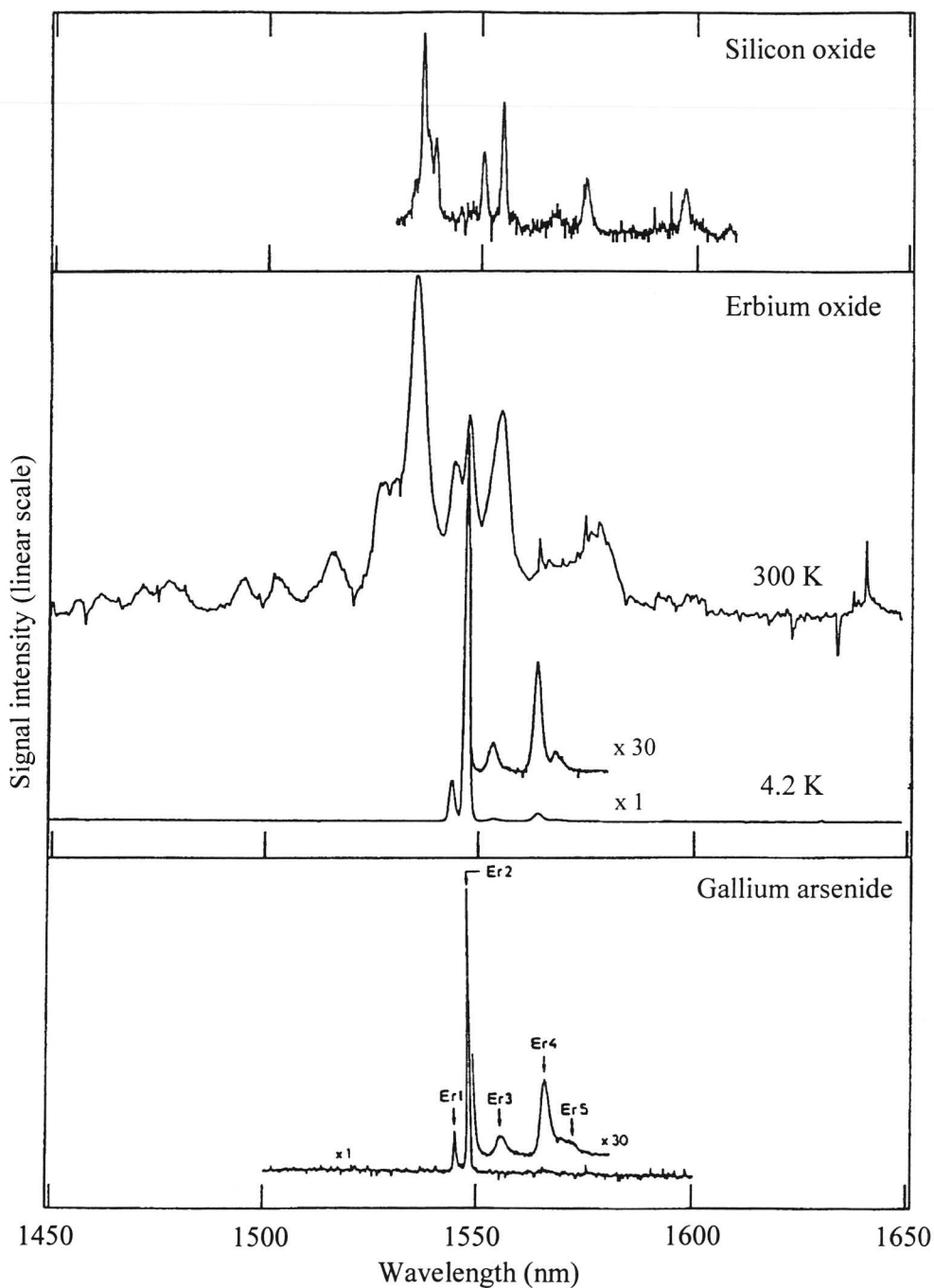
Figure 2.3 *Photoluminescence spectra of silica:Er at 4.2 K, erbium oxide at 4.2 K and 300 K, and GaAs:Er at 4.2 K (after [2.4]).*

luminescence, so surface defects will play an important role in the luminescence process. The luminescence of the bulk defects, which can be seen at higher temperatures, could be effectively absorbed at low temperatures by the surface defects. The erbium ion is very attractive to oxygen ions [2.8], so only a small amount of oxygen in the annealing process will be sufficient to oxidise some of the erbium at the surface of the GaAs crystal to form Er_2O_3 surface defects.

The main luminescence-active defect in Cz Si and SiO_2 samples is the erbium-related one with lines A, D, F, H and K as described by Tang *et al.* [2.2]. Also the main lines B, C, E and G, ascribed in the literature as due to a non-cubic defect [2.2, 2.12], can be seen in figure 2.2. In SiO_2:Er the defects seem to have the same intensity; both defects show a strong dependence on the presence of oxygen, which is supported by the EXAFS measurements [2.3, 2.8]. EXAFS has revealed that erbium, both in silica and Cz silicon, has oxygen ligands as nearest neighbours. Combination of these two observations leads to a model of an erbium atom on a cubic site surrounded by six oxygen atoms as most probable structure for the main luminescent defect in Czochralski silicon and in silica.

These measurements are in agreement with the observations of Coffa *et al.* [2.13]. They discuss the presence of luminescent erbium on two sites: one that dominates at high temperatures, with short lifetimes and oxygen involvement which relates well to our "A, D, F, H, K" defect and the other one which matches our "B, C, E, G" defect. They also observed that only a small percentage of the erbium was luminescent, consistent with our observation of long luminescence decay times and saturation of the signal with increasing laser intensity. The spectrum of FZ Si:Er consists of one broad band and at least 5 other lines of comparable intensity; the symmetry of the luminescent erbium centre must thus be lower than cubic. The splitting between the outermost lines A and F is only 36 nm indicating a relatively weak crystal field. This is consistent with the structure as found with EXAFS [2.8].

2.4.2 Phonon replicas

It appears that, to a good accuracy, the energy differences between the positions of several luminescence lines are equal. An equal separation is observed for Cz Si:Er between the A and D and the D and F lines, respectively; in the case of SiO_2 this holds even for the series of four lines A, D, F, and a very small one appearing as a high-energy shoulder of H. The lines in these series react similarly to changes of temperature, chopper frequency, etc. In view of these spectral features a new explanation of the origin of these luminescence lines as phonon sidebands is suggested. The spectroscopic positions of these lines are well described

38

by the assumption of a local phonon of 9.6 meV of energy. On a similar basis, a local phonon of 35 meV for ytterbium in indium phosphide has been reported [2.5].

In the local-phonon model the following theoretical predictions have to be satisfied:

- At low temperatures, $kT \ll \hbar\Omega$, where $\hbar\Omega$ is the energy of the local phonon which dominates the luminescence band, the side band involving n phonons of any frequency has the relative intensity

$$I_n = S^n \exp(-S)/n!. \tag{2.1}$$

Equation (2.1) gives the transition probabilities in terms of the dimensionless parameter S, known as the Huang–Rhys factor [2.14]. At the same time, the width of the replicas will increase with the number of phonons created.

- At elevated temperatures a new line will appear in the luminescence spectrum at the high-energy side of the zero-phonon line with the same energy difference as the local phonon replicas: the anti-Stokes line. The intensity ratio of the anti-Stokes line and the first local phonon side band is

$$\frac{I_{(\omega+\Omega)}}{I_{(\omega+\Omega)}} = \exp\left(\frac{-\hbar\Omega}{k_B T}\right) \tag{2.2}$$

where ω is the zero-phonon luminescence frequency and Ω is the frequency of the phonon being emitted or absorbed [2.15] .

Figure 2.4 illustrates the spectra for Cz Si observed at 4.2, near 50, and near 100 K showing the phonon side bands of the Stokes and anti-Stokes type. Table 2.2 gives a summary of the experimental and theoretical intensities of the phonon replicas at the lower energies for the different values of n. In silica:Er three phonon replicas can be observed which fit well with a Huang–Rhys factor $S = 0.63$, representing a weak coupling. For Cz Si:Er the analysis is more complicated because the two no-phonon lines are overlapping. Michel *et al.* give a high-resolution spectrum (figure l(a) in Ref. 2.6) that shows also three replicas and fit with $S = 0.729$. Not only good agreement with the theoretical intensity variation, but also a fair similarity between silica and Czochralski silicon is achieved.

At elevated temperatures a line which can be identified as the anti-Stokes replica is observed. Its measured intensity relative to the first phonon-emission mode is near 0.5 for both Cz Si and SiO$_2$. For the temperature of the measurement, which is at an estimated 100 to 120 K,
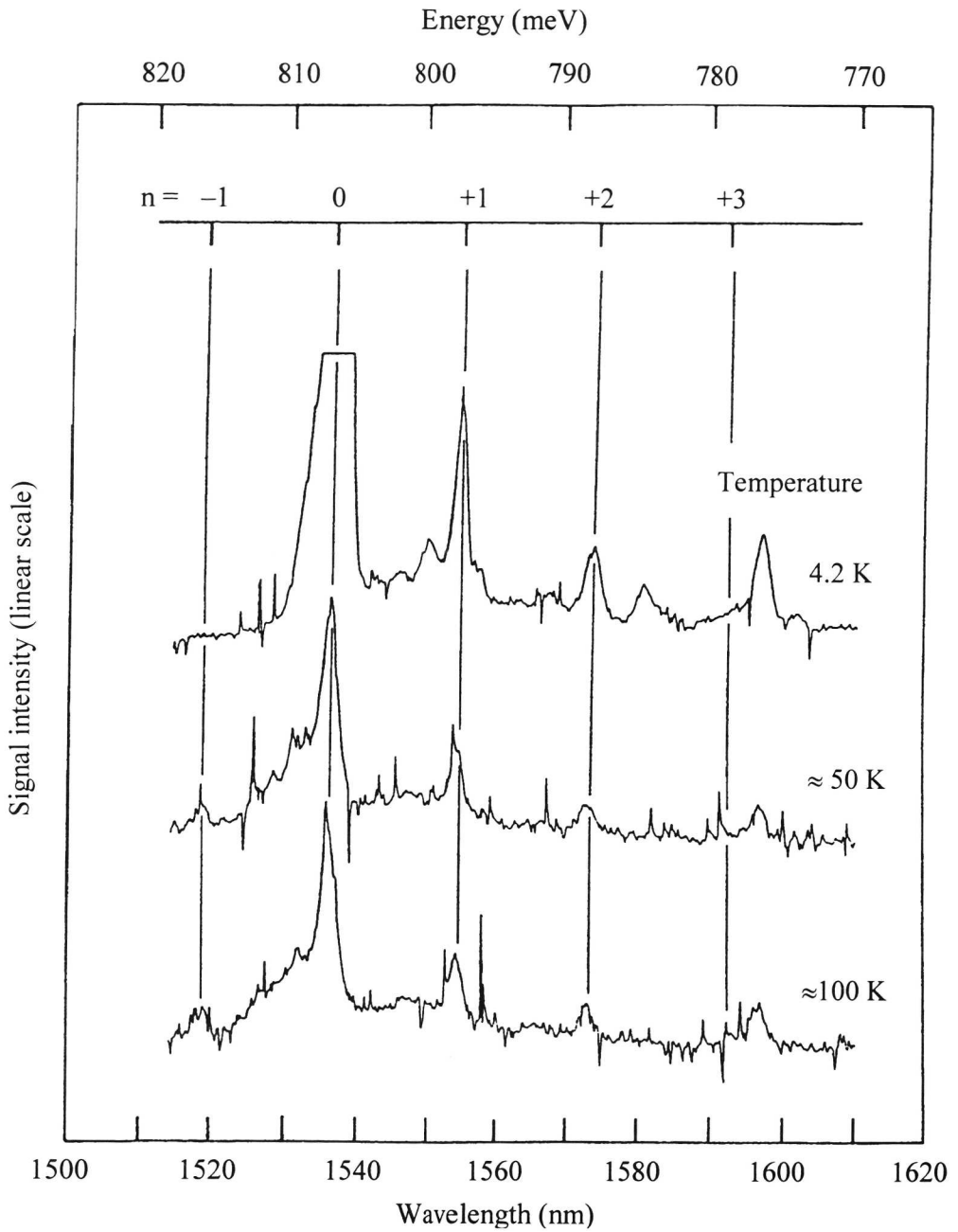
Figure 2.4 *Photoluminescence spectra of Cz Si:Er measured at 4.2 K, near 50 K and near 100 K, with phonon replica structure indicated.*

equation (2.2) requires the ratio to be near 0.4. The agreement provides support to the proposed model of identifying major features of the PL spectrum as phonon side bands.

Table 2.2 *Theoretical (th), experimental (exp) and calculated (calc) intensities I_n of the n-th phonon replicas relative to the zero-phonon line n = 0: I_n/I_0, for erbium-related luminescence. S is the Huang–Rhys factor.*

Sample		I_1/I_0	I_2/I_0	I_3/I_0	Reference
	th	S	$S^2/2$	$S^3/6$	[2.14]
Cz Si	exp	0.729	0.212	0.047	[2.6]
	calc	0.729	0.265	0.064	
Cz Si	exp	0.265	0.09		This work
	calc	0.265	0.04		
SiO$_2$	exp	0.63	0.27	0.045	This work
	calc	0.63	0.20	0.042	

2.4.3 Crystal-field analysis

The phonon side band model accounts for the position of several lines; in table 2.3 the assignments are listed. Further structure of the spectra could be related to crystal-field splitting of the ground state having $J = 15/2$. Following Lea *et al.* [2.16] the cubic crystal-field Hamiltonian is expressed as

$$\mathcal{H} = WxO_4/60 + W(1-|x|)O_6/13860. \tag{2.3}$$

O_4 and O_6 are the fourth- and sixth-order crystal-field operators, x determines the ratio of the fourth- and sixth-order coefficients and has a value in between -1 and +1. x fixes the mutual distance and sequence of the five levels; the calculated levels scale with W, see section 1.5.4.
The best fit to the lines not yet accounted for in the phonon replica model for Cz-Si:Er was obtained with $x = -0.85$ and $W = 1.068$ cm^{-1} (0.132 meV). In this range of x the lowest level of the first excited state is of Γ_8 character; in this case it is expected that all five lines are present in the emission spectrum. Calculations based on the four strongest lines showed a deviation of 4 cm^{-1} (0.5 meV) between calculation and experiment. The fifth, weakest, line was then expected at 1668 nm but found at 1672 nm, at a difference of 14 cm^{-1} (1.7 meV). This magnitude of discrepancy is common for similar studies [2.12, 2.17]; it is normally

ascribed to the neglect of the influence of the higher-lying J multiplets. The value of x means that the erbium atom has T_d symmetry in the lattice with the perturbing atoms in fourfold co-ordination.

With the values as found for x and W, the difference between the lowest two levels of the excited state multiplet $^4I_{13/2}$ is calculated to be 38 cm^{-1} (4.7 meV). This provides a satisfactory explanation for the appearance, at higher temperatures, of the so-called hot lines with an about 5 meV higher energy. The hot-line assignments are included in table 2.3.

It should be emphasised that the present crystal-field analysis is based on a different set of lines as previously used in the literature [2.12] and consequently leads to different results for the parameters. The selection of a proper set of lines in one spectrum does not seem to be unique with the present state of characterisation of the lines. Future research, for example including Zeeman studies or optically detected magnetic resonance (ODMR), is required for an unambiguous interpretation of the spectra. Such studies are currently in progress.

Since the observed defect of Er_2O_3 seems to be cubic and the five lines in this defect are all well defined, this spectrum is a perfect candidate for application of theoretical calculations of the crystal field parameters. The best fit to all observed data was obtained with $x = 0.45$ and $W = 0.28$ cm^{-1}.

Table 2.3 *Photoluminescence spectra of Cz Si:Er, measured at 4.2 K and 77 K, with assignments.*

Label	Wavelength (nm)	Energy (meV)	Assignment
	1517.8	816.9	Anti-Stokes line
	1528.5	811.2	Hot-line of A
	1529.9	810.4	Hot-line of B
A	1536.9	806.7	No-phonon line of cubic defect (1)
B	1538.2	806.0	No-phonon line of non-cubic defect
	1546	802.0	Line of cubic defect (2)
	1547	801.5	Hot-line of D
C	1550.7	799.5	Line of non-cubic defect
D	1555.3	797.2	Phonon replica of A (9.5 meV)
E	1568.2	790.6	Line of non-cubic defect
F	1574.6	787.4	Second phonon replica of A
G	1581.4	784.0	Line of non-cubic defect
H	1597.8	776.0	Line of cubic defect (3)
I	1602.7	773.6	Line of non-cubic defect
K	1642.8	754.7	Line of cubic defect (4)
M	1667	743.8	Line of cubic defect (5)

2.5 Conclusion

In conclusion, it appears that in both Cz Si and SiO_2 erbium is surrounded by, most probably, oxygen atoms as nearest neighbours. The same complex is formed irrespective of the abundance of oxygen in silicon oxide or the relatively low concentration near 10^{-5} in Czochralski silicon. It seems that to great extent, regardless of the host material, erbium dopant forces its immediate environment into a well defined oxygen-rich cluster, possibly of high cubic symmetry.

References

[2.1] H. Ennen, J. Wagner, H.D. Müller and R.S. Smith, J. Appl. Phys. **61** (1987) 4877.

[2.2] Y.S. Tang, K.C. Heasman, W.P. Gillin and B.J. Sealy, Appl. Phys. Lett. **55** (1989) 432.

[2.3] M.A. Marcus and A. Polman, J. Non-Cryst. Solids **136** (1991) 260.

[2.4] F. Bantien, E. Bauser and J. Weber, J. Appl. Phys. **61** (1987) 2803.

[2.5] H. Ennen and J. Schneider, *Proc. Thirteenth Int. Conf. on Defects in Semiconductors,* ed L.C. Kimerling and J.M. Parsey Jr (Warrendale, Pennsylvania: The Metallurgical Society of AIME) 1985 pp. 115–127.

[2.6] J. Michel, L.C. Kimerling, J.L. Benton, D.J. Eaglesham, E.A. Fitzgerald, D.C. Jacobson, J.M. Poate, Y.-H. Xie and R.F. Ferrante, Mater. Sci. Forum **83–87** (1992) 653.

[2.7] A. Polman, D.C. Jacobson, D.J. Eaglesham, R.C. Kistler and J.M. Poate, J. Appl. Phys. **70** (1991) 3778.

[2.8] D.L. Adler, D.C. Jacobson, D.J. Eaglesham, M.A. Marcus, J.L. Benton, J.M. Poate and P.H. Citrin, Appl. Phys. Lett. **61** (1992) 2181.

[2.9] R.M. Moon, W.C. Koehler, H.R. Child and L.J. Raubenheimer, Phys. Rev. **176** (1968) 722.

[2.10] J.B. Gruber, J.R. Henderson, M. Muramoto, K. Rajnak and J.G. Conway, J. Chem. Phys. **45** (1966) 477.

[2.11] G.H. Dieke, *Spectra and Energy Levels of Rare Earth Ions in Crystals,* ed H.M. Crosswhite and H. Crosswhite (New York: Interscience Publishers, 1968) p. 294.

[2.12] H. Przybylinska, J. Enzenhofer, G. Hendorfer, M. Schoisswohl, L. Palmetshofer and W. Jantsch, Mater. Sci. Forum **143–147** (1994) 715.

[2.13] S. Coffa, G. Franzò, F. Priolo, A. Polman and R. Serna, Phys. Rev. B **49** (1994) 16313.

[2.14] G. Davies, Phys. Rep. **176** (1989) 83.

[2.15] C. Kittel, *Introduction to Solid State Physics,* 6th edn (New York: John Wiley and Sons, Inc, 1986) p. 306.

[2.16] K.R. Lea, M.J.M. Leask and W.P. Wolf, J. Phys. Chem. Solids **23** (1962) 1381.

[2.17] J.D. Kingsley and M. Aven, Phys. Rev. **155** (1967) 235.